

Ferritin-bound Platinum Nanoparticles in Hydrogen Production

Matthew Dalton Richards

A thesis report submitted to the faculty of

Brigham Young University

In partial fulfillment of the requirements for the degree of

Bachelor of Science

John S. Colton, Advisor

Department of Physics and Astronomy

Brigham Young University

April 2019

Copyright © 2019 Matthew Dalton Richards

All Rights Reserved

ABSTRACT

Ferritin-bound Platinum Nanoparticles in Hydrogen Production

Matthew Dalton Richards

Department of Physics and Astronomy

Bachelor of Science

Hydrogen gas has been hailed as the fuel of the future. Unfortunately, significant problems with its production, storage, and transportation prevent its widespread use. One possible solution is to make hydrogen gas using ferritin-bound platinum nanoparticles (FBPNs). I studied the optimum time of UV exposure for making FBPNs, and the ability of FBPNs to synthesize hydrogen gas. FBPN samples were made by reacting chemicals under a UV lamp with stirring. I fractionated the FBPN samples using size-exclusion chromatography and the fraction with the FBPNs was identified using spectrophotometry. I tested the protein concentration using the Lowry protein assay and the platinum concentration using ICP-MS. Using these results, the number of platinum nanoparticles per ferritin was calculated. I then used the FBPNs to catalyze hydrogen gas production. The amount of hydrogen gas was tested using TCD-GC. Preliminary results indicate that the optimum time for production of FBPNs is 30 minutes of UV exposure, resulting in 182.7 platinum nanoparticles per ferritin being formed. I successfully synthesized hydrogen gas as well. While difficulties with the LPA make the results tenuous, the methods, with some modification, would allow the quick analysis of other important parameters in this process and should be pursued.

Keywords: Ferritin, Platinum, Nanoparticles, Hydrogen

Acknowledgments

I'd like to thank my parents for teaching me to work hard and give it my all. I couldn't have finished this thesis without the tenacity their teaching instilled. I'd like to thank my advisor Dr. John S. Colton for his mentoring. The research was ultimately successful in no small part due to his encouragement and physics wisdom. Dr. Colton also kindly reviewed multiple drafts of this thesis. I'd also like my lab partners Daniel Boyce and Chapman Lindsay. The research couldn't have been completed without their keen insight and excellent work.

Table of Contents

Table of Contents	vi
List of Figures.....	ix
■ Introduction.....	10
<i>1.1 Motivation.....</i>	<i>10</i>
<i>1.2 Background and Prior Work.....</i>	<i>12</i>
1.2.1 Platinum	12
1.2.2 Ferritin.....	13
1.2.3 Methyl-Viologen.....	15
1.2.4 Previous Work at BYU	16
<i>1.3 Overview</i>	<i>17</i>
■ Methods.....	18
<i>2.1 Existing Methods.....</i>	<i>18</i>
2.1.1 FBPN Creation.....	18
2.1.2 FBPN Characterization	19
<i>2.2 Background.....</i>	<i>19</i>
2.2.1 SEC	19
2.2.2 Spectrophotometry.....	20
2.2.3 LPA.....	20
2.2.4 ICP-MS	21

2.2.5	TCD-GC.....	21
2.3	<i>Experimental Procedure</i>	22
2.3.1	Synthesizing FBPNs.....	24
2.3.2	Implementing SEC.....	26
2.3.3	Implementing Spectrophotometry.....	27
2.3.4	Implementing LPA.....	28
2.3.5	Implementing ICP-MS.....	28
2.3.6	Calculating Number of Platinum Nanoparticles per Ferritin.....	28
2.3.7	Synthesizing H ₂	29
2.3.8	Implementing TCD-GC.....	30
■	Results, Summary, and Future Work.....	31
3.1	<i>Results</i>	31
3.1.1	UV Exposure.....	31
3.1.2	Platinum Nanoparticles per Ferritin.....	32
3.1.3	TCD-GC.....	33
3.2	<i>Discussion</i>	34
3.3	<i>Summary and Future Work</i>	36
	Appendix A.....	39
	<i>Platinum Ion Elution</i>	39
	Appendix B.....	40
	<i>Protein Testing</i>	40

Appendix C	43
<i>Absorbance of the Fractions at 280 nm</i>	43
■ Index	45
References	46

List of Figures

Figure 1.1 Hydrogen production methods	11
Figure 1.2 Schematic of ferritin	14
Figure 1.3 Schematic of methyl-viologen	16
Figure 2.1 Size-exclusion chromatography	20
Figure 2.2 Simplified Diagram of TCD-GC	22
Figure 2.3 Experimental sequence	24
Figure 2.4 UV lamp setup	26
Figure 2.5 Gel column setup	27
Figure 3.1 Color change after UV exposure	32
Figure 3.2 Platinum nanoparticles per ferritin	33
Figure 3.3 Hydrogen gas per platinum.....	34
Figure 3.4 Lowry protein analysis results	35
Figure A.1 Platinum ion elution in the absence of ferritin.....	39
Figure B.1 Protein standard curve.....	41
Figure C.1 Absorbance of the fractions at 280 nm	43
Figure C.2 Absorption profile of platinum ions	44

■ Introduction

1.1 Motivation

Hydrogen gas has been hailed as the energy source of the future because of its advantages over fossil fuels. Fossil fuel production is controlled by a handful of nations, and fossil fuels will be depleted in the near future. Fossil fuel combustion also releases noxious chemicals into the atmosphere causing poor air quality in major cities. Hydrogen gas, by contrast, is ubiquitously available and can be renewable. Hydrogen's only byproduct from combustion is water.

Hydrogen is also a more versatile energy source. Fossil fuels are exclusively combusted to release their energy, but hydrogen gas can be reacted in a chemical fuel cell as well.¹ Chemical fuel cells create electricity directly from reacting the hydrogen gas. Recognizing these benefits, countries around the world see hydrogen as an important renewable fuel for the future.

Unfortunately, most hydrogen gas currently is not renewably produced. Most hydrogen gas is produced by the steam reforming of fossil fuels as shown in Fig. 1.1.² Steam reforming is a high temperature and high pressure reaction of water with fossil fuels to produce hydrogen gas. Hydrogen gas can be made in other ways, but the technology and resources are lacking. Electrolysis, for example, is a great way to make hydrogen gas, but the necessary electricity mainly comes from fossil fuels. Scientists are researching other, renewable methods, but currently most hydrogen is made in non-renewable ways.

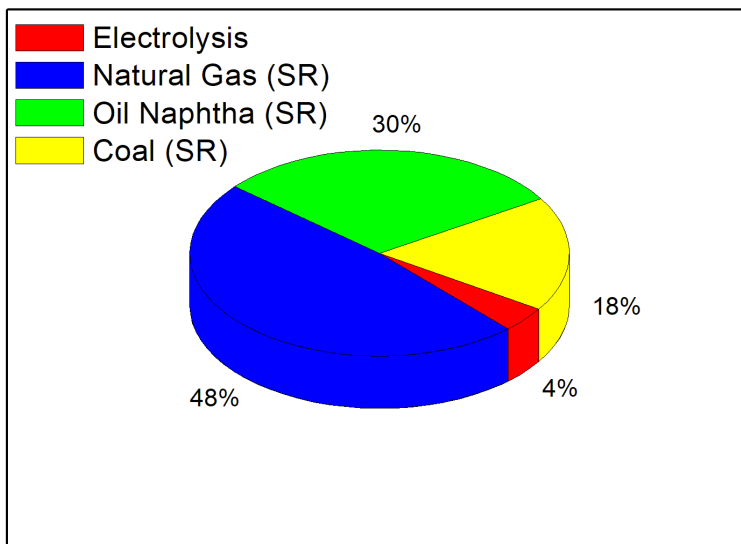


Figure 1.1 Hydrogen production methods. (SR) indicates steam reforming. Natural gas, oil naphtha, and coal are all fossil fuels. Hydrogen production by electrolysis is the only method not directly involving fossil fuels. However, the electricity used for electrolysis typically comes from fossil fuel sources. Current hydrogen production is non-renewable. Data from Ref. 2.

In addition to problems with renewable production, transporting and storing hydrogen gas—an inherent part of utilizing any fuel—presents more difficulties. Hydrogen gas has high energy per mass density. However, it is not very dense.^{2,3} In order to increase density for transportation, hydrogen must be liquefied. Unfortunately, liquid hydrogen rapidly boils off. Boil-off can be as high as 3% per day for liquefied hydrogen.¹ Boil-off is a problem for even short-term storage and transportation.

Ferritin-bound platinum nanoparticles (FBPNs) present a possible solution to these problems. FBPNs produce hydrogen gas in a renewable way, independent of fossil fuels.⁴ Using FBPNs, hydrogen can safely be made at or near the point of use—something impossible to do with steam reforming. Hydrogen gas can also be made as needed, alleviating the need for expensive and ineffective storage.

The process of making and using FBPNs needs is promising, but needs more refinement. There are two parts to this process. First, ferritin is exposed to UV light in the presence of platinum ions to make platinum nanoparticles. Then, in a separate reaction, these FBPNs—in conjunction with methyl-viologen—are exposed to UV light, catalyzing the production of hydrogen gas. The current concentrations of hydrogen gas made using this process are not high enough for fuel use. This process has many unexplored parameters, which could increase the hydrogen gas yield. Parameters include the optimum time of UV exposure for FBPN synthesis, the optimum time of exposure for hydrogen gas production, and the optimum concentrations of reactants.

In this thesis, I explore the optimum UV exposure time for making FBPNs. I also explore the ability of these nanoparticles to make hydrogen gas. Preliminary results indicate that 30 minutes of UV exposure is the optimal time for nanoparticle production. Hydrogen gas was also successfully synthesized.

1.2 Background and Prior Work

1.2.1 Platinum

Platinum is a catalyst for many chemical reactions. A catalyst is a substance that helps a chemical reaction happen but is not incorporated into the products, or the yield, of the reaction. Platinum is commonly used in the oil industry for fractioning crude oil into its various parts. Platinum also catalyzes the breakdown of hydrogen peroxide, the oxidization of glucose, the formation of hydrogen gas, and the hydrogenation of vegetable oils, just to name a few reactions.⁵

While bulk platinum is a good catalyst, platinum nanoparticles are in some cases an even better catalyst. Platinum nanoparticles catalyze the same reactions at safer temperatures and pressures.⁶ They are also recyclable which is notable because some catalysts do not recycle well.

Platinum nanoparticles show increased catalytic ability because of their unique properties. The large surface area of platinum nanoparticles allows more chemical reactions to nucleate on the surface as compared to bulk platinum.⁷ In some chemical reactions, experiments have shown platinum nanoparticles produce 10 to 100 times more product than bulk platinum at the same atomic concentration.^{4,7}

1.2.2 Ferritin

In our process, platinum nanoparticles are made using ferritin. Ferritin is an important protein in iron metabolism, serving as both as iron storage and as an iron detoxifier.⁸ Ferritin is spherical in shape and weighs about 474,000 Daltons (a Dalton is a common unit of measure for proteins and is equivalent to the AMU) as shown in Figure 1.2. The protein shell of ferritin is 12 nm in outer diameter and 8 nm in inner diameter. Iron is stored in the inner cavity as a ferrihydrite mineral, $\text{Fe}(\text{O})\text{OH}$. These iron cores vary in size from a few iron atoms up to 4500 iron atoms.

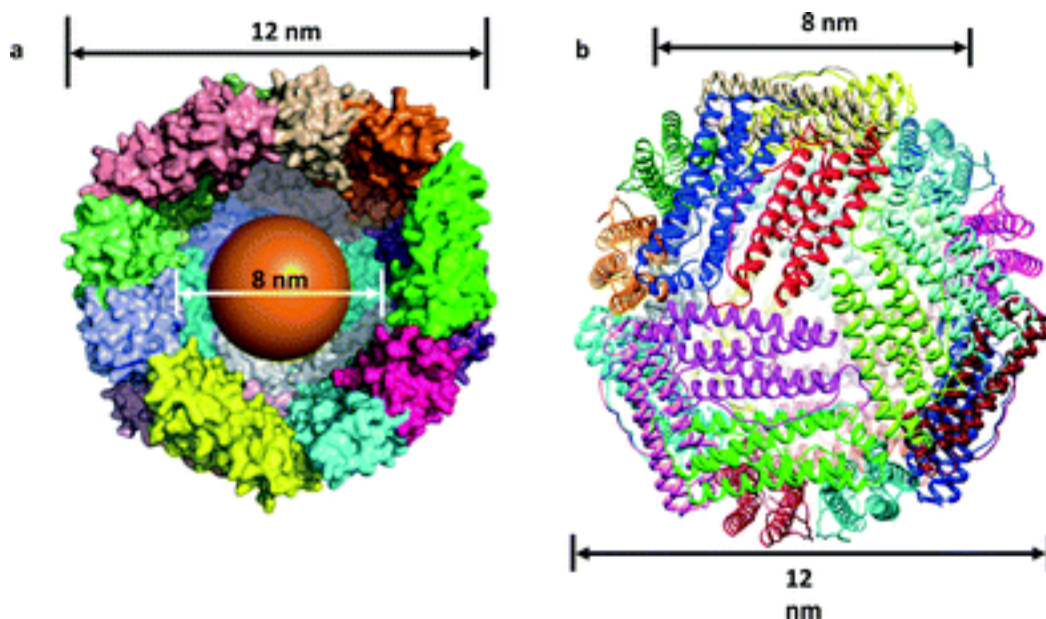


Figure 1.2 Schematic of ferritin. a) A cutaway of ferritin with the iron mineral core in the center (brown sphere). b) Protein structure of ferritin. Reproduced from Ref. 9 by permission from the Royal Chemical Society.

Ferritin has a number of useful properties for chemical reactions and nanoparticle synthesis. Ferritin is stable up to 80° C and can withstand pH levels from 5-10 without significant degradation.⁹ In addition, ferritin is soluble under many conditions, making it quite versatile in various chemical reactions.

One of the most important properties of ferritin is its photo-reducing capabilities. Photo-reducers are substances that reduce or give an electron to other chemicals upon illumination. Ferritin can photo-reduce because of its iron oxide mineral core.¹⁰ The core is a semiconductor with a direct band gap of 3.053 eV and an indirect band gap of 2.14 eV.¹¹ Upon illumination of ferritin with UV light, electrons are excited to the conduction band of the semiconductor core. The protein shell transfers the excited electrons to the outside of ferritin. The free electrons then reduce the species outside of the ferritin. With a proper electron donor present in the solution with ferritin, the hole in the valence-band of the semiconductor core is filled, and the process

repeats. By using ferritin as a photo reductant, a variety of materials have been reduced including chrome, copper, cytochrome c, thiol compounds, viologens, and platinum.^{12,13}

1.2.3 Methyl-Viologen

Methyl-viologen is an electron transfer catalyst in light-harvesting reactions. If excited with light, it can accept electrons—becoming reduced—and then donate those electrons to other substances. Methyl-viologen consists of a double benzene ring with nitrogen atoms replacing two carbon atoms as shown in Figure 1.3a. Two methyl groups are attached to the nitrogens. Methyl-viologen is used in light harvesting reactions as shown in Fig. 1.3b. Initially, methyl-viologen (MV^{2+}) is reduced when illuminated in the presence of an electron donor. In its reduced

form (MV^+) and in the presence of a catalyst like platinum nanoparticles, methyl-violgen (MV^+) reduces hydrogen ions into hydrogen gas.^{14,15,16}

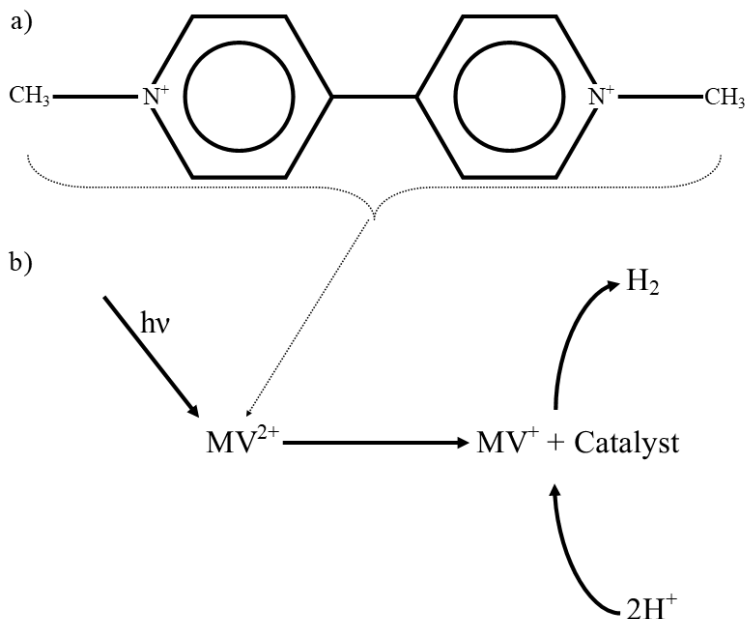


Figure 1.3 Schematic of methyl-violgen. a) Methyl-violgen (MV^{2+}) consists of two benzene rings with nitrogen atoms replacing carbon atoms as shown. Methyl groups (CH_3) are attached to the nitrogen. b) Methyl-violgen is reduced (MV^+) by illumination ($h\nu$) in the presence of an electron donor (electron donor not pictured). Methyl-violgen (MV^+) can then reduce, with the aid of a catalyst, hydrogen ions (H^+) into hydrogen gas (H_2).

1.2.4 Previous Work at BYU

Previous work at BYU has been fruitful. Dr. David Petrucci, in his PhD dissertation, describes using FBPNs to produce hydrogen gas in a two-part process.⁴ First, he used ferritin to reduce platinum ions into platinum nanoparticles. The 1-2 nm diameter nanoparticles were dispersed on the outside of ferritin. He then used these nanoparticles to catalyze hydrogen gas formation. With methyl-violgen acting as an electron shuttle, an electron donor such as oxalate or citrate, and the FBPNs as a catalyst, hydrogen ions were reduced into hydrogen gas. He

produced hydrogen gas in amounts up to 25,000 ppm, or 25,000 H₂ molecules per million air molecules. The FBPNs produced 10 to 100 times more hydrogen gas than bulk platinum at the same atomic concentration.

1.3 Overview

Continuing on Petrucci's work, I investigated the optimal UV exposure time for making FBPNs and the FBPNs' ability to catalyze hydrogen production. I successfully produced FBPNs and hydrogen gas. The highest yield of nanoparticles was at 30 minutes UV exposure with 182.7 nanoparticles per ferritin being formed. Unfortunately, this result seems implausible at present because of difficulties with the Lowry protein assay (LPA). The highest yield of hydrogen gas was 9,000 ppm.

The upcoming chapters discuss the methods and results. In Ch. 2, I discuss the concentrations and methods for producing FBPNs. I also discuss the methods used to characterize the FBPNs and hydrogen gas: size-exclusion chromatography (SEC), spectrophotometry, Lowry protein assay (LPA), inductively-coupled plasma mass spectroscopy (ICP-MS), and thermal conductivity detection gas chromatography (TCD-GC). I discuss the results in Ch. 3, giving emphasis to the next steps in this project. My methods, with the inaccuracies of the LPA fixed, will allow quick testing of other reaction parameters not tested in this thesis and can be used for further exploration.

■ Methods

This chapter contains a review of existing methods for making and characterizing ferritin-bound platinum nanoparticles (FBPNs), the background of those methods, and how those methods were implemented.

2.1 Existing Methods

2.1.1 FBPN Creation

Existing methods for the formation of FBPNs were to my knowledge solely developed by Petrucci. I used his concentrations and some of his methods.

Petrucci used the following concentrations and methods to create FBPNs. His reaction consisted of 150 $\mu\text{g/mL}$ ferritin, 2 mM Pt^{2+} , 50 mM NaCl, 30 mM Tris, and 30 mM sodium citrate. These chemicals were reacted in a temperature-controlled cuvette with stirring under a UV lamp. Various times of UV exposure and various temperatures were tested.

He analyzed nanoparticle synthesis by spectrophotometry and transmission electron microscopy (TEM). Using a spectrophotometer, he measured the absorbance of the sample. He found that as the nanoparticles formed, they caused a change in the absorbance spectrum. Using TEM, he directly imaged the platinum nanoparticles. He found the platinum nanoparticles were spherical, 1 to 2 nm in diameter, and congregated on the outside of the ferritins.

After making the nanoparticles, he used them to synthesize hydrogen gas. His base method consisted of FBPNs, methyl-viologen, and an electron donor in an acidic medium

(acidity is a measure of H^+ ions). These chemicals were put into a sealed vial and degassed. The chemicals were reacted under a UV lamp with stirring. Various times of UV exposure were tested. He then measured the hydrogen concentration using thermal-conductivity detection gas chromatography (TCD-GC).

2.1.2 FBPN Characterization

Methods for investigating nanoparticles include size-exclusion chromatography (SEC), Lowry protein assay (LPA), and inductively-coupled plasma mass-spectroscopy (ICP-MS).¹⁷ After synthesizing nanoparticles, SEC is used to separate chemicals by size. Most importantly, SEC can separate proteins from smaller particles like ions and salts. LPA tests for protein concentration. ICP-MS tests for metal concentration. By combining these methods, the number of platinum nanoparticles per ferritin can be calculated.

2.2 Background

I chose to use SEC, spectrophotometry, LPA, ICP-MS, and TCD-GC to characterize the FBPNs and the hydrogen gas made using the FBPNs. A brief explanation of these methods is given below.

2.2.1 SEC

SEC is used to separate chemicals by size. A typical SEC setup is shown in Figure 2.1. A typical SEC setup is a plastic column filled with hydrated gel-beads. The gel-beads (blue spheres) act as a reverse filter of sorts; smaller particles (purple spheres) get trapped by the gel-beads, while larger particles (red spheres) pass through the column without interacting with the gel-beads. A buffer (like Tris) is used to help the sample through the column. As the buffer and

the separated chemicals pass (elute) through the column, they are collected in 1.0 or 1.5 mL amounts called fractions.

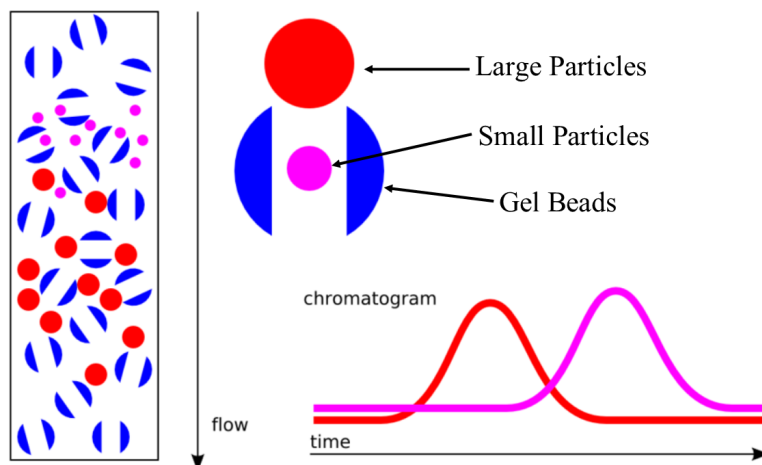


Figure 2.1 Size-exclusion chromatography. SEC separates chemicals into different bands based on size. Depending on the type of gel beads (blue spheres), large particles (red spheres) would be excluded from the beads and elute faster than small particles (purple spheres). Wikipedia Commons.

2.2.2 Spectrophotometry

Spectrophotometry is used to find the absorbance of a sample at specific wavelengths. Initially, light is sent through a grating. The grating selects an individual wavelengths of light. The selected wavelength is then sent through the sample, and the intensity of the transmitted light is measured. The sample intensity is corrected by subtracting the intensity of transmitted light from a standard called a blank (usually water).

2.2.3 LPA

The Lowry protein assay (LPA) is used to find protein concentration.¹⁸ The LPA is a complicated chemical reaction. Initially, a reagent denatures the protein. The peptide bonds of the protein chelate Cu^{2+} (also in the initial reagent), causing Cu^{+1} to form. The Folin-Ciocalteu

reagent is then added. The Cu^+ complex then reduces this reagent, causing it to turn blue. The amount of reduction is proportional to the number of peptide bonds, and thus the amount of protein. The bluer a sample solution is after performing the LPA, the more protein there is. This color change can quantitatively be measured using the absorbance at 750 nm. A standard curve is prepared using known concentrations of proteins. A sample with unknown concentration is compared to this standard curve to find the protein concentration.

2.2.4 ICP-MS

ICP-MS is used to test for the concentration of metal atoms. Initially, a sample is ionized into ions. The ions are directed by sets of four rods who have alternating electric fields being applied to them. These sets of rods are called quadrupoles. These quadrupoles shape the electric field to only allow certain ions—based on their charge-to-mass ratio—to interact with the ion detector. When ions interact with the ion detector, it causes an electrical response. Just like with LPA, this electrical response is compared against a standard curve and the concentration of metal atoms is deduced. The standard curve is made using the electrical response of samples with known concentrations of metal atoms.

2.2.5 TCD-GC

TCD-GC is used to measure the concentration of gases. TCD-GC consists of two main components: separation and thermal conductivity detection. The process is shown in Figure 2.2. Initially, a gas sample is injected into a heated chromatographic column. The column causes different gases to flow at different rates, causing gases to separate much like a gel column does with liquids. A carrier gas is used to push the sample gas through the column. The separated gases are then sent through a thermal conductivity detector. The detector consists of resistors

sensitive to changes in temperature. Depending on the thermal conductivity of the gas (as compared to the carrier gas), the resistors change resistance. The change in resistance causes a voltage response which is recorded on a chromatogram. The area under the voltage response is calculated and compared to the area under the voltage response for known concentrations of gases. Using this, the gas concentration is deduced.

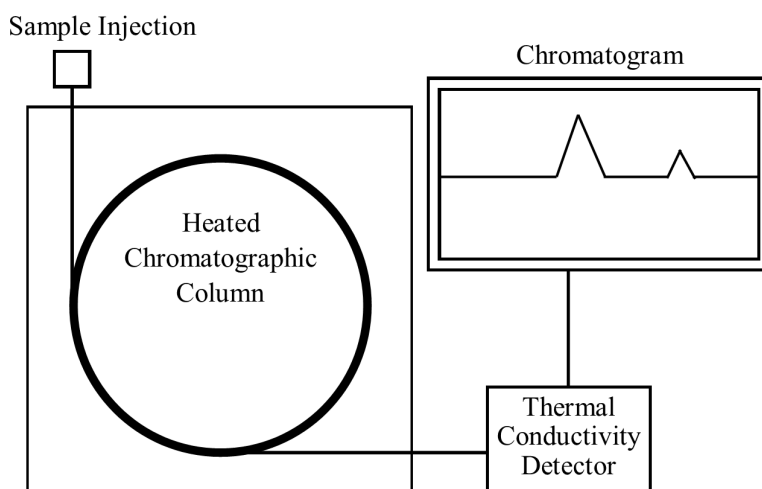


Figure 2.2 Simplified Diagram of TCD-GC. Initially a gas sample is injected into the column. The column causes the various gases to separate. After separation, the gases are sent through a thermal conductivity detector. The varying thermal conductivity of the gases causes a voltage response and a chromatogram is produced. The voltage response is integrated and compared to known concentrations. Using this information, the unknown gas concentration is found.

2.3 Experimental Procedure

My first goal was to find the optimal time of UV exposure for nanoparticle synthesis. I used Petrucci's concentrations as discussed in Section 2.1.1 because I did not want concentrations to be a confounding variable. I used most of Petrucci's methods for making FBPNs, but I did not control the temperature of the reaction like Petrucci because I wanted to ensure the reaction was robust to changes in temperature. However, I did monitor the

temperature to make sure that the reaction did not get hot enough ($\sim 80^{\circ}\text{C}$) to degrade ferritin.

The details of synthesis are discussed in Section 2.3.1.

With my goal of finding the optimal UV exposure time, I needed to measure the number of nanoparticles per ferritin formed. I used SEC, spectrophotometry, LPA, and ICP-MS to find the number of platinum nanoparticles per ferritin. These are discussed in Section 2.3.2-2.3.6.

My second goal was to see if I could produce hydrogen gas in similar concentrations to Petrucci. I used Petrucci's concentrations and methods for making hydrogen gas. I analyzed the concentration of hydrogen gas using TCD-GC. The synthesis and characterization of hydrogen gas are discussed in Section 2.3.7-2.3.8.

An outline of my experimental sequence is shown in Fig. 2.4.

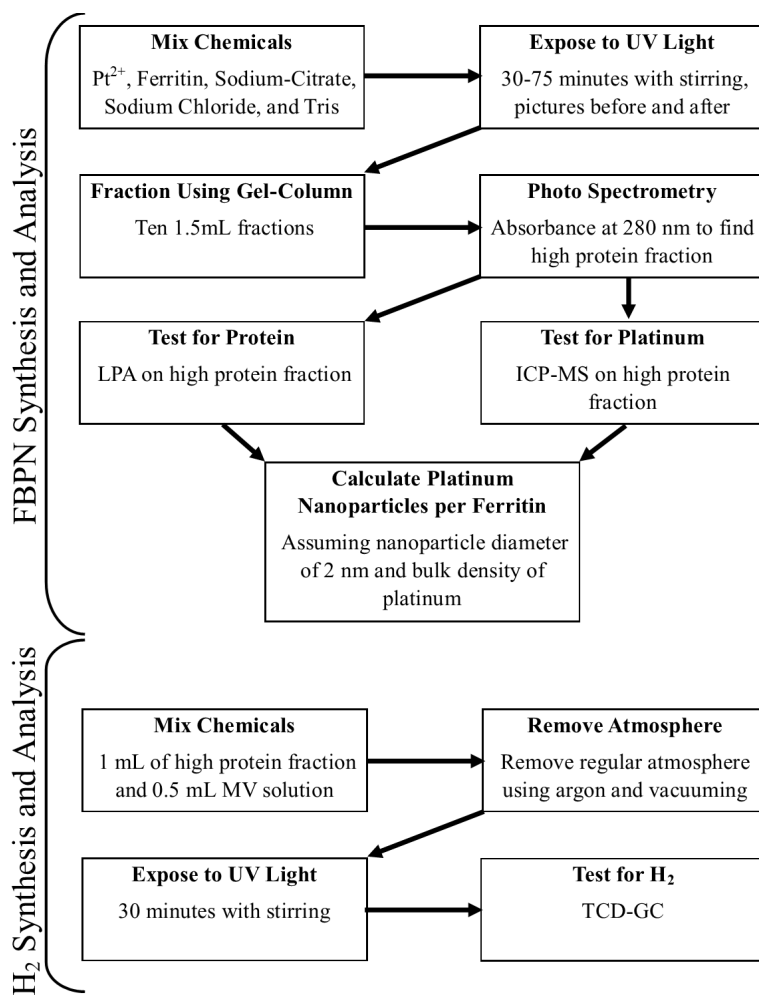


Figure 2.3 Experimental sequence. My experiment consisted of two parts: synthesizing and analyzing FBPNs and synthesizing and analyzing H₂.

2.3.1 Synthesizing FBPNs

FBPNs were formed in the following way. I combined 2 mL of each of the following: 750 µg/mL ferritin (made fresh to prevent protein degradation), 10 mM Pt²⁺ (made using PtCl₄), 250 mM NaCl, 150 mM Tris (pH 7.4), and 150 mM sodium citrate. Thus, the reaction concentrations were: 150 µg/mL ferritin, 2 mM Pt²⁺, 50 mM NaCl, 30 mM Tris, and 30 mM sodium citrate. A stir bar was added and the chemicals were briefly stirred.

I separated the 10 mL mixture into four 2 mL samples. I put the samples in 3.5 mL screw cap septum vials (Thermo Fisher Scientific). I threw away the remaining 2 mL of mixture. The samples were then exposed to UV light, with stirring, for 30, 45, 60, and 75 minutes. Photos of the samples were taken before and after UV exposure to catalogue the color change.

During some of my reactions, I monitored the temperature of my reaction. I used a J-type thermocouple to monitor the temperature. I covered the thermocouple end with parafilm and placed it into the vial. I recorded the temperature every 5 minutes. The temperature never exceeded 50°C (well below the degradation temperature of ferritin).

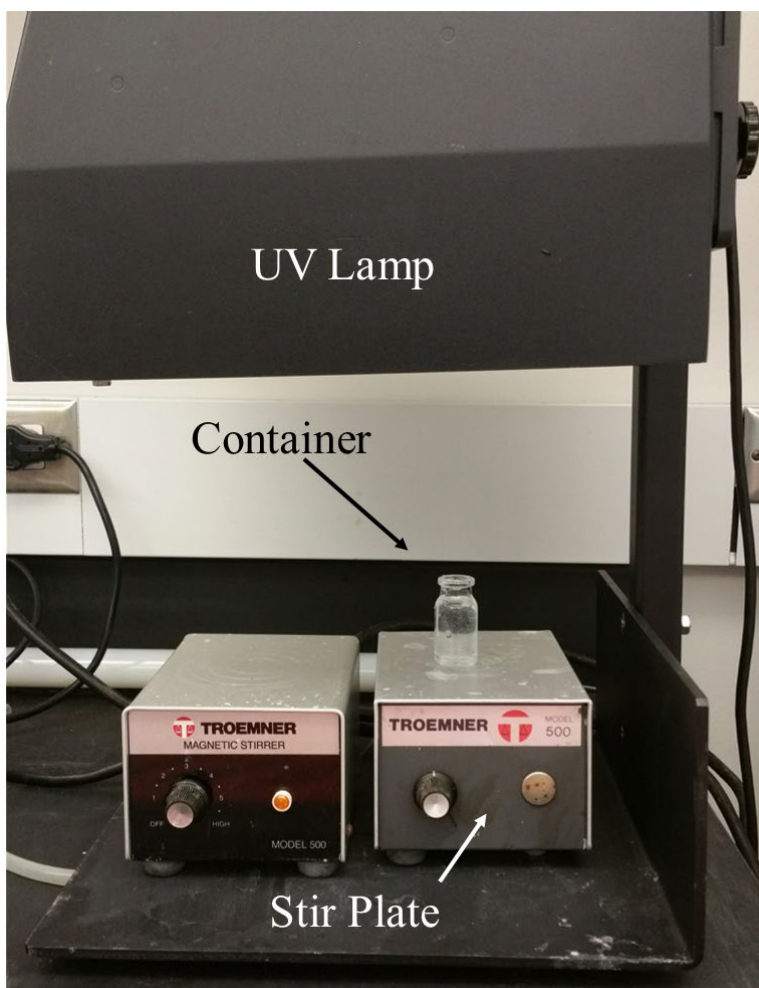


Figure 2.4 UV lamp setup. This setup was used to make FBPNs. When exposing samples to UV light, a UV shield was used (not pictured). The lamp is a Sunray 400 High Power UV Flood Lamp (Integrated Dispensing Solutions) and was run at full power.

2.3.2 Implementing SEC

After the four 2 mL samples were made, they were fractionated using SEC in order to separate ferritin (with nanoparticles attached) from unbound platinum ions. To prepare and use the column, I used the method found in the appendix of Kameron Hansen's senior thesis.¹⁹ The gel-column for SEC consisted of a 1 cm diameter column filled with ~10 cm of Sephadex G-100 gel-beads (Fig. 2.4). The gel was held in place by two filter discs. Tris (30 mM at pH 7.4) was used to elute the sample through the column. As explained in Appendix A, between runs I flushed the column with 10 mL of Tris to remove unwanted chemicals. I collected ten 1.5 mL fractions in 1.5 mL Eppendorf tubes, for a total volume collected of 15 mL (Thermo Fisher Scientific).

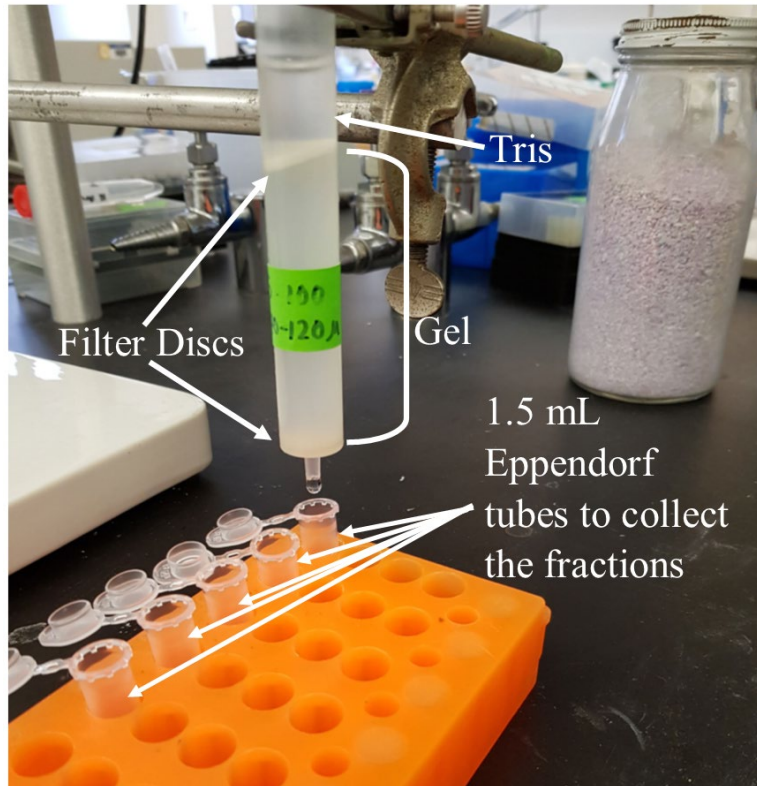


Figure 2.5 Gel column setup. The gel column consists of a column 1 cm in diameter filled with ~10 cm of gel held in place by 2 filter discs. The sample is placed on the top and elutes through the column as illustrated in Figure 2.1. As the sample drips out of the column, it is collected in the 1.5 mL Eppendorf tubes. I used Tris to help the sample elute through the column, and I collected 10 fractions of 1.5 mL each. The column separated ferritin (with nanoparticles attached) from unbound platinum ions.

2.3.3 Implementing Spectrophotometry

I then measured the absorbance of the fractions at 280 nm to identify the fraction with the highest protein concentration. The absorbance at 280 nm is indicative of protein concentration. The spectrophotometer lamps needed to warm up for 30 minutes before taking measurements. I blanked the spectrophotometer using a water filled cuvette. I rinsed the cuvette with milli Q water between every fraction, and every five fractions I got a new cuvette.

2.3.4 Implementing LPA

Next, the protein concentration of the highest absorbance fraction was tested using LPA as discussed in Section 2.2.3. I used the micro-well plate protocol. A useful discussion about protein methods and protocols is found in Appendix B. The instructions for the micro-well plate protocol are found in the Watt lab Standard Operating Procedures. The absorbance can be measured using the micro-well plate reader in room E240 of the Benson. My standard curve was prepared using 2 mg/mL bovine serum albumin (BSA) diluted in water (Sigma Aldrich). My standard curve consisted of duplicate samples with 0-10 μg of BSA.

2.3.5 Implementing ICP-MS

Next, the platinum concentration of the highest absorbance fraction was tested using ICP-MS as discussed in Section 2.2.4. The details of preparing samples and standards for ICP-MS use are found in the appendix of Kameron Hansen's senior thesis.¹⁹ Each fraction was tested in duplicate for a more reliable result: two test tubes with 40 μL of sample each. The standards for the calibration curve were prepared by performing a serial dilution with a 1 ppm platinum standard (Millipore Sigma). The standard was diluted using 2.5% v/v hydrochloric acid. Standards of 0, 200, 400, 600, 800, and 1000 ppb platinum (μg platinum per kg total mass) were prepared and used.

2.3.6 Calculating Number of Platinum Nanoparticles per Ferritin

Using the results from LPA and ICP-MS, I calculated the number of platinum nanoparticles per ferritin in the high protein fraction. Using the concentration (X $\mu\text{g}/\text{mL}$) of this fraction, the number of ferritins was calculated:

$$\frac{1.5 \text{ mL}}{\text{fraction}} \times \frac{X \text{ } \mu\text{g}}{1 \text{ mL}} \times 1 \text{ mol ferritin} \times 4.74 \times 10^{11} \text{ } \mu\text{g} \times \frac{6.022 \times 10^{23} \text{ ferritins}}{1 \text{ mol ferritin}} = \# \text{ of ferritins in fraction} . \quad (1)$$

Assuming an average diameter of 2 nm (based on Petrucci's results), the average mass of an individual nanoparticle was found:

$$\frac{4}{3} \pi (1 \times 10^{-7} \text{ cm})^3 \times \frac{2.143 \times 10^4 \text{ } \mu\text{g platinum}}{\text{per cm}^3} = \text{mass of nanoparticle} (=8.98 \times 10^{-17} \text{ } \mu\text{g}) . \quad (2)$$

Using the ICP-MS results (Y ppb or $\mu\text{g}/\text{kg}$) of this fraction and the average mass of a nanoparticle (Eq. (2)), the number of platinum nanoparticles in the fraction was calculated:

$$\frac{Y \text{ } \mu\text{g}}{\text{kg}} \times \frac{1.5 \times 10^{-3} \text{ kg}}{\text{fraction}} \times \frac{1}{\text{mass of nanoparticle (} \mu\text{g)}} = \# \text{ of platinum nanoparticles in fraction} . \quad (3)$$

The number of platinum nanoparticles per ferritin is the ratio of Eqs. (1) and (3):

$$\frac{\# \text{ of platinum nanoparticles in fraction}}{\# \text{ of ferritins in fraction}} = \# \text{ of platinum nanoparticles per ferritin} . \quad (4)$$

2.3.7 Synthesizing H₂

The FBPNs, made and characterized, were then used to make hydrogen gas. The reaction happened in a sealed vial with 1 mL of the high protein fraction and 0.5 mL of a stock solution. The vial was a 3.5 mL screw cap septum vial (Thermo Fisher Scientific). The stock solution consisted of 60 mM methyl-viologen, 150 mM NaCl, and 450 mM sodium citrate at a pH of 4. The container was degassed using the method outlined in Kameron Hansen's senior thesis.¹⁹ The regular atmosphere was replaced with argon. After the vial was degassed, it was reacted under the UV lamp with stirring for 30 minutes as shown in Figure 2.4.

2.3.8 Implementing TCD-GC

Next, the concentration of hydrogen gas was tested using TCD-GC (See 2.2.5). The TCD-GC machine is in S-125 ESC and is operated by Dr. Zou of the Food Science Department. Hydrogen gas leaks out quickly, even in sealed vials. Because of this, I tested the vials immediately after reacting them under the UV lamp. To do this, I would coordinate a time with Dr. Zou to test the sample. I would react my samples and bring them to Dr. Zou right after finishing. Dr. Zou would then immediately test the samples.

■ Results, Summary, and Future Work

In this chapter, I present the results of a final run of my experiment. As noted before, the results show that the optimal UV exposure time for FBPN synthesis is 30 minutes, but as will be discussed in Section 3.2, this result doesn't seem plausible. I discuss my findings and give some direction to future work.

3.1 Results

3.1.1 UV Exposure

The color change of the FBPNs samples indicates the formation of platinum nanoparticles. With UV exposure, the samples changed from light brown to dark brown as shown in Figure 3.1. These changes are consistent with other platinum nanoparticle experiments; a change from light to dark brown indicates the formation of platinum nanoparticles.²⁰

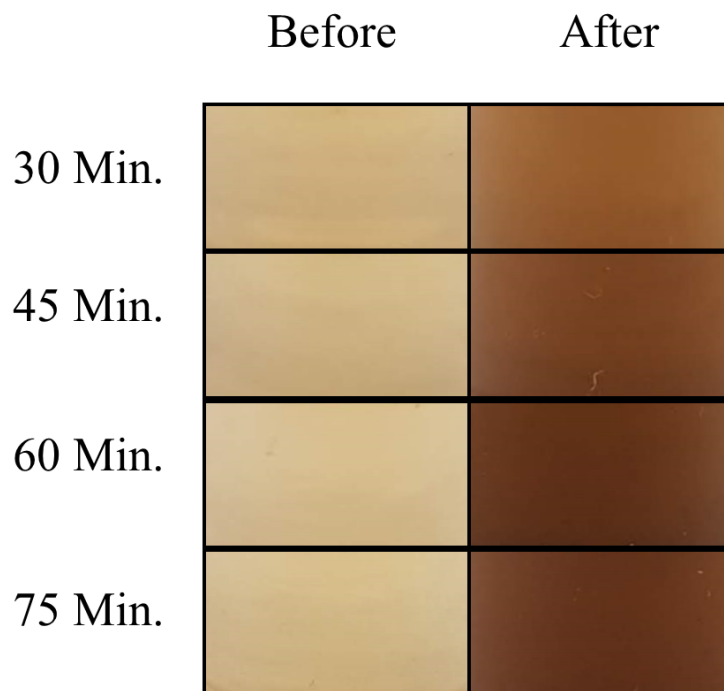


Figure 3.1 Color change after UV exposure. This was made using the cropped photos of the samples. Color change is indicative of platinum nanoparticle formation. There is no noticeable difference in the final color of the 45, 60, and 75 minute samples. However, they are all darker than the 30-minute sample. This indicates that more nanoparticles are being formed after 30 minutes of UV exposure.

3.1.2 Platinum Nanoparticles per Ferritin

Using the results from LPA and ICP-MS, I calculated the number of platinum nanoparticles per ferritin as discussed in Section 2.3.6. The number of platinum nanoparticles per ferritin for various UV exposure times is shown in in Figure 3.2. The calculated maximum amount of platinum nanoparticles per ferritin was 182.7, which occurred with 30 minutes of UV exposure. Based on the TEM images from Petrucci’s work, the calculated number of platinum nanoparticles per ferritin seems quite high. This result is based on the assumption that platinum nanoparticles are on average 2 nm in diameter. These results suggest the assumption that the

nanoparticles are on average 2 nm in diameter may be false. In addition, problems with the LPA casts further doubt on this result as will be discussed in Section 3.2.

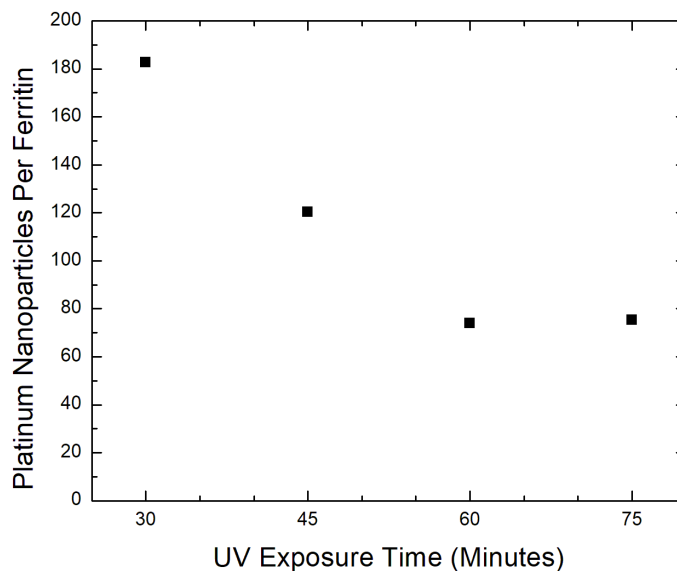


Figure 3.2 Platinum nanoparticles per ferritin. The details of the calculations are discussed in Section 2.3.6. The highest amount of platinum nanoparticles per ferritin was 30 minutes. The number of platinum nanoparticles decreased with increasing exposure time until reaching a minimum at 60 minutes UV exposure.

3.1.3 TCD-GC

Using the fraction with the highest amount of protein for each exposure time, I synthesized hydrogen gas as explained in Section 2.3.7 and measured the amount of hydrogen gas as explained in Section 2.3.8. Since each of the highest fractions had a different amount of platinum in it, I normalized the TCD-GC results by dividing by the amount of platinum as shown in Figure 3.3. The 30 minutes UV exposure FBPNs were the most catalytically active, producing 0.17 ppm of hydrogen gas for every ppm of platinum ions.

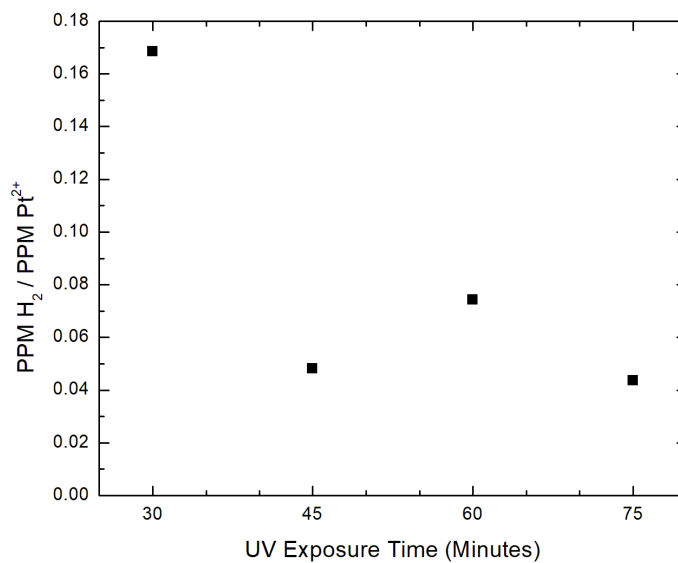


Figure 3.3 Hydrogen gas per platinum. The amount of hydrogen gas produced was normalized by dividing by the amount of platinum ions in the high protein fraction for each UV exposure time. The FBPNs made from 30 minutes UV exposure were the most catalytically active.

3.2 Discussion

According to the results, the optimal time of UV exposure is 30 minutes, but this should be taken with caution. The Lowry protein assay (LPA) was problematic. While ferritin may vary in which fractions it elutes, no fraction should have more protein than was put into the column. For each exposure time, there was 300 μg of ferritin in the sample. That would be the expected maximum amount of ferritin present in any fraction. Based on the reasonable assumption that about two-thirds of the ferritin elutes in one fraction, roughly 200 μg of protein would be expected. Unfortunately, the LPA found protein concentrations higher than 300 μg in 3 of the highest absorbance fractions as shown in Fig. 3.4. This makes the results of the LPA

questionable. The resulting calculation of the number of platinum nanoparticles per ferritin is also questionable. This makes drawing conclusions about the optimal UV exposure time tenuous.

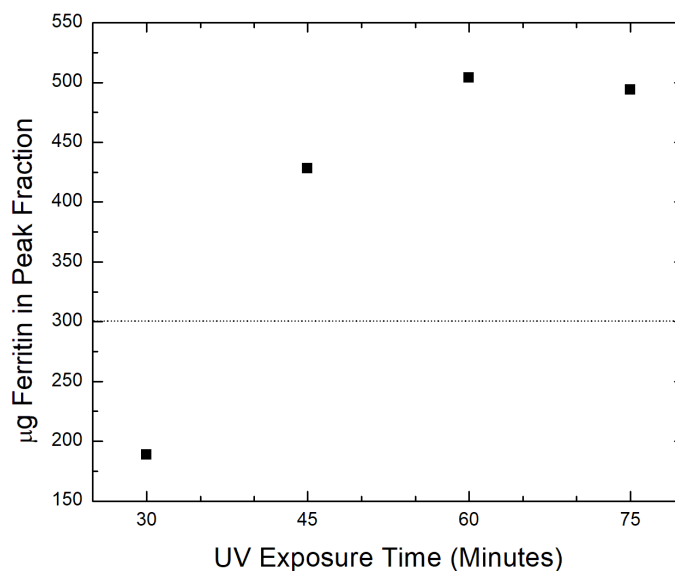


Figure 3.4 Lowry protein analysis results. No fraction should have more than 300 µg of protein (dashed line is the 300 µg mark). Unfortunately, according to the LPA, the high protein fraction of 45, 60, and 75 minutes of UV exposure had more protein than this. This makes the LPA results and the resulting calculations of platinum nanoparticles per ferritin questionable.

While the optimal UV exposure time is difficult to discern from LPA and ICP-MS results, the TCD-GC results may resolve the situation. Normalized for the amount of platinum present, 30 minutes of UV exposure produced the most hydrogen gas. Thirty minutes UV exposure may be the best time for producing the most catalytic FBPNs.

There is a possible reason for why 30 minutes UV exposure resulted in the most catalytically active FBPNs, and that reason may explain a couple of the other results. Catalysts must interact with the reactants for reactions to occur. In a liquid phase reaction, catalysts more readily interact with liquid reactants if the catalyst is in solution. Ferritin keeps the FBPNs

soluble, allowing them to freely interact with H^+ ions. If Ferritin was degraded or the FBPNs became detached, the FBPNs would lose some of their catalytic ability. With continued UV exposure, Ferritin may be breaking down (See Appendix C), and the FBPNs may lose some of their catalytic ability.

3.3 Summary and Future Work

I successfully made FBPNs and produced hydrogen gas using them. I found that 30 minutes was the optimum UV exposure time, but that result is tenuous. This amount of UV exposure produced platinum nanoparticles with a concentration of 182.7 nanoparticles per ferritin. I also successfully produced hydrogen gas.

However, I did not make platinum nanoparticles nor hydrogen gas in the amounts that Petrucci did. As noted before, the results are questionable because the LPA results are inaccurate. A complete retest with corrections to the LPA would be worth pursuing: it may lead to obtaining similar results to Petrucci.

In addition to a complete retest, many parameters could be explored with our current method. In particular, varying the pH—the concentration of free protons—may lead to higher concentrations of hydrogen gas. The hydrogen gas reaction utilizes the free protons in the acidic medium. As the reaction progresses, the protons are consumed to form hydrogen gas. As the concentration of free protons decreases, the production of hydrogen gas slows. Decreasing the pH (increasing the number of free protons) would allow more hydrogen gas to be formed. However, a low pH could have negative effects on other components of the system. By testing various pH levels, a happy medium could potentially be found.

Another parameter worth investigating is the concentration of sodium citrate. During the synthesis of FBPNs, sodium citrate allows the semiconductor core of ferritin to continue reducing platinum forming nanoparticles. As the concentration of sodium citrate depletes, the semiconductor core oxidizes, and the formation of platinum nanoparticles slows or stops. By varying the concentration of citrate, an optimal concentration could be found.

There are also possibilities beyond the current method worth pursuing. Novel core ferritin is one such possibility. The native core of ferritin can be replaced with different cores.¹⁹ These cores could have properties better suited for nanoparticle synthesis. The bandgap of novel cores, for example, is sometimes smaller than native cores. With a smaller bandgap, visible light could excite electrons instead of only UV light. This would allow platinum nanoparticles to be formed without a UV lamp. In addition, the novel cores may more readily donate electrons leading to more platinum nanoparticles per ferritin being formed.

Another interesting possibility is mixed metal nanoparticles. One group found that platinum-palladium nanoparticles showed greater catalytic ability than both platinum and palladium nanoparticles by themselves.²¹ Petrucci also made palladium nanoparticles using ferritin just like platinum nanoparticles.⁴ A reaction with both palladium and platinum ions could result in a mixed-metal nanoparticle. Using the methods in this thesis, these mixed-metal nanoparticles could be characterized and tested for catalytic ability.

The methods developed for this project are easily replicable. Although this thesis represents the culmination of nearly two years of research, the results presented in this thesis come from a final test of the procedure that took two weeks. If LPA difficulties are resolved,

then any number of parameters could quickly and easily be tested and the process could be further refined.

Appendix A

Platinum Ion Elution

Since samples are often run through the gel-column one after another, if platinum ions are left in the column, they will elute with the next sample. To test if platinum is left in the column, I put a 1.5 mL sample of 2 mM Pt^{2+} (made from PtCl_4) through the gel-column and took 25 1 mL fractions. The platinum concentration of the fractions was then tested using ICP-MS. The ICP-MS results are shown in Figure A.1. A majority of the platinum ions elute after the volume FBPNs fractions are typically collected as indicated by the dashed line at 15 mL. Because of this result, I decided to flush the gel column with 10 mL of Tris (30 mM, pH 7.4) between every run to ensure platinum ions were not left in the column.

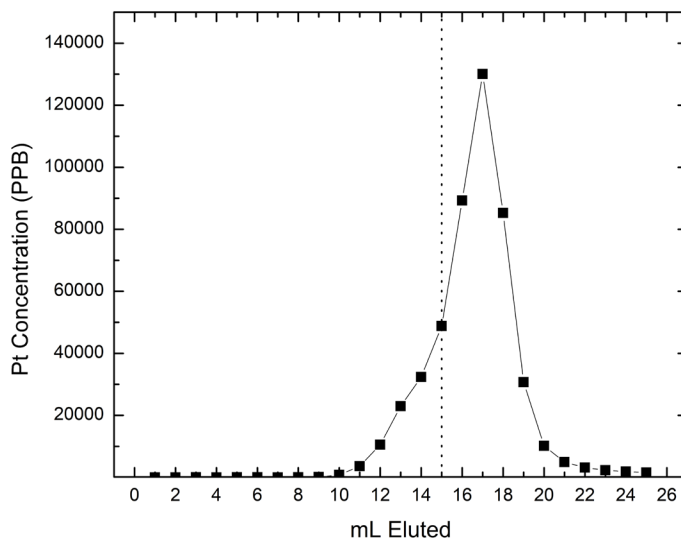


Figure A.1 Platinum ion elution in the absence of ferritin. The dashed line is the volume at which we stop collecting fractions with FBPN samples. Most of the platinum ions come out after that line. Without clearing out the column, the left over platinum ions would have eluted with the next FBPN sample, obscuring the actual platinum elution of the next sample.

Appendix B

Protein Testing

There are two methods of protein testing I considered using for this research, each of which have strengths and weaknesses. The Lowry protein assay (LPA), the method used in this thesis, is in general the most accurate method for protein quantification.²² Unfortunately, the results of the LPA can be affected by other chemicals present in a solution. Specifically, Tris can alter the amount of protein detected by the LPA.²³ The Bradford protein assay (BPA), on the other hand, isn't affected by other chemicals in the solution.²⁴ However, it is less accurate. Also, because how each protein reacts to the BPA reagent is unique, standard curves must be prepared using the same protein that will be tested. For example, if samples containing ferritin will be tested using the BPA, the standard curve needs to be prepared using ferritin, not bovine serum albumin (BSA).

Both BPA and LPA methods were considered, but in the end, I decided that LPA was better for our work. First and foremost, the LPA is more accurate. While LPA is affected by other chemicals in the solution, the effects are mostly negligible for the concentrations we are working with. In addition, the effects of the other chemicals can be accounted for by preparing the protein solutions for the standard curve using the offending chemicals.

With the LPA selected as the type of protein testing, a specific protocol must be selected. In general, the more sample the protocol requires for testing, the more accurate the protocol will be. Thus, protocols that use more sample should be selected. I used the micro-well plate protocol because it is fast and easy, but there are other protocols that use more sample volume and are

probably more accurate²⁵. Future students might find better results using one of these higher volume protocols.

Preparing a standard curve is the next consideration. The standard curve prepared and used in this research is shown in Fig. B.1. The response of protein to the LPA is linear over short ranges. Standard curves with smaller ranges of protein concentration are more accurate for response within that range. Before preparing the standard curve, it is best to consider what the protein concentration of the sample that will be tested might be. Based on the LPA results of the 30 minutes UV exposure sample as seen in Fig. 3.2, a reasonable assumption when collecting in 1.5 mL fractions is that two thirds of the protein elutes in the fraction with the highest absorbance at 280 nm. Using this assumption, the protein concentration can be calculated. The standard curve should then be prepared so that the assumed concentration of the sample is in the middle of the standard curve.

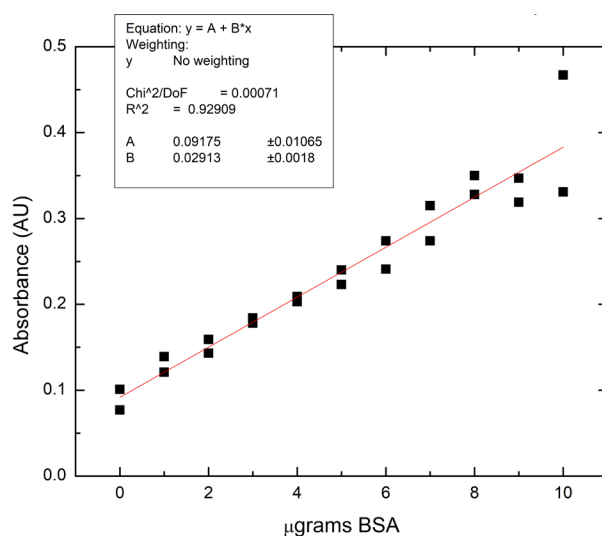


Figure B.1 Protein standard curve. This standard curve was used to deduce the protein concentration in the high protein fractions. The protein response is linear over short ranges.

Appendix C

Absorbance of the Fractions at 280 nm

After separation the samples using size-exclusion chromatography (SEC), the absorbance of the fractions at 280 nm was tested. The absorbance at 280 nm for the four samples is shown in Figure C.1. The absorbance was measured to find the fraction with most of the protein. For all exposure times, the fraction with the highest absorbance at 280 nm was the 6 mL fraction. Interestingly, there was an increase in absorbance in later fractions. This secondary peak isn't from the protein, which elutes earlier. Also, the 6 mL peak increased with increased UV exposure.

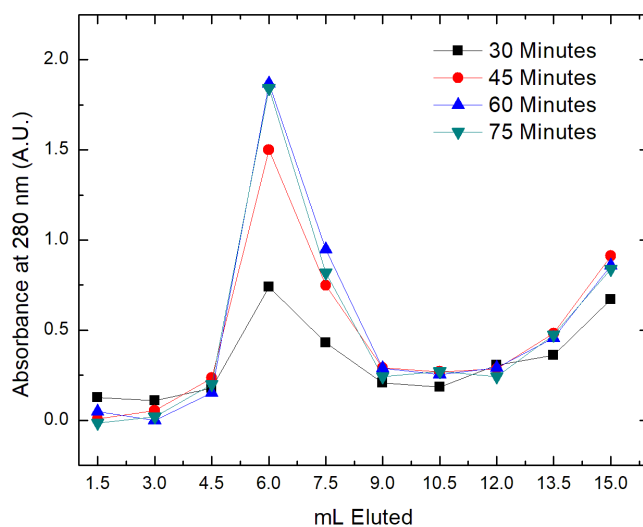


Figure C.1 Absorbance of the fractions at 280 nm. The large first peak at 6 mL is the high protein fraction. This fraction was tested further, and using the results, the number of platinum nanoparticles per ferritin was calculated. Interestingly, the 6 mL peak increases further UV exposure. In addition, there is a secondary peak. Platinum nanoparticles and platinum ions may explain both of these trends.

Platinum ions and platinum nanoparticles may explain both of these trends. I measured the absorbance of 2 mM Pt^{2+} on the spectrophotometer. The absorbance profile is shown in Figure C.2. Platinum ions have a small but non-negligible absorption at 280 nm. In addition, platinum nanoparticles have absorbance peaks around 280 nm²⁰. With prolonged UV exposure, more platinum nanoparticles could have formed, causing an increase in the size of the 6 mL peak.

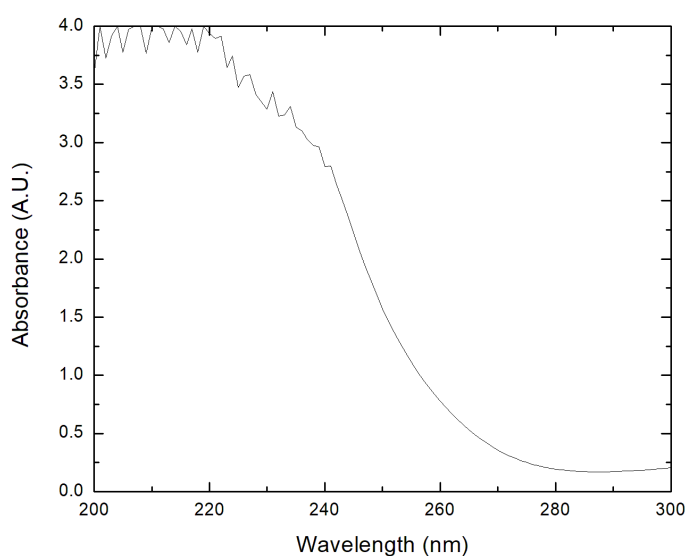


Figure C.2 Absorption profile of platinum ions. Platinum ions have a small but non-negligible absorption at 280 nm. This may in part explain the secondary absorbance peak in the fractions shown in Figure C.1.

Index

- argon, 29
- benzene, 15, 16
- catalytic, 13, 35, 36, 37
- catalytically. *See* catalytic, *See* catalytic
- Dalton, 13
- elute, 20, 26, 27, 39, 42
- FBPNs, iii, 11, 12, 16, 17, 18, 19, 22, 24, 26, 29, 31, 33, 34, 35, 36, 37, 39
- ferritin, iii, ix, 12, 13, 14, 16, 17, 18, 19, 23, 24, 25, 26, 27, 28, 29, 32, 33, 34, 35, 36, 37, 39, 40, 42, 45
- Ferritin-bound Platinum Nanoparticles, i, iii
- gel-beads, 19, 26
- gel-column, 26, 39
- inductively-coupled plasma mass-spectroscopy, 19
- methyl-viologen, ix, 12, 15, 16, 18, 29
- mineral core, 14
- novel core, 37
- photo-reducers, 14
- platinum nanoparticles, iii, 11, 12, 13, 16, 18, 19, 23, 28, 29, 31, 32, 33, 35, 36, 37, 42, 43, 45
- quadrupoles, 21
- semiconductor, 14, 37
- size-exclusion chromatography, iii, 17, 19, 42
- spectrophotometer, 18, 27
- steam reforming, 10, 11
- thermal conductivity detection gas chromatography, 17
- transmission electron microscopy, 18
-

References

- ¹ S. Singh et al., "Hydrogen: A sustainable fuel for future of the transport sector," *Renewable & Sustainable Energy Reviews* 51, 623-633 (2015).
- ² S. Banerjee, M. N. Musa, and A. B. Jaafar, "Economic assessment and prospect of hydrogen generated by OTEC as future fuel," *Hydrogen Energy* 42, 26-37 (2017).
- ³ S. Sharma and S. K. Ghoshal, "Hydrogen the future transportation fuel: From production to applications," *Renewable & Sustainable Energy Reviews* 43, 1151-1158 (2015).
- ⁴ O. D. Petrucci, "Ferritin-Based Photo-Oxidation of Biomass for Nanoparticle Synthesis, Bioremediation, and Hydrogen Evolution," *All These and Dissertations*. Paper 4308.
- ⁵ J. Fan et. al., "Direct evidence for catalase and peroxidase activities of ferritin-platinum nanoparticles," *Biomaterials* **32**, 1611-1618 (2011).
- ⁶ G. Zhiqiang, et. al., "Controlled hydrogenation of aromatic compounds by platinum nanowire catalysts," *RSC Advances* 8, 3477-3480 (2012).
- ⁷ M. Shao, A. Peles, and K. Shoemaker, "Electrocatalysis on Platinum Nanoparticles: Particle Size Effect on Oxygen Reduction Reaction Activity," *Nano Letters* **11**, 3714-3719 (2011).
- ⁸ P. M. Harrison and P. Arosio, "Ferritins: Molecular properties, iron storage function and cellular regulation," *Biochimica et Biophysica Acta* 1275, 161-203 (1996).
- ⁹ R. K. Watt, et al., "Ferritin as a model for developing 3rd generation nano architecture organic/inorganic hybrid phot catalysts for energy conversion," *Catalysis Science & Technology* 3, 3103-3110 (2013).
- ¹⁰ I. Kim, et al., "Photochemical reactivity of ferritin for Cr(VI) reduction," *Chemistry of Materials* 14, 4874-4879 (2002).
- ¹¹ J. S. Colton, et al., "Sensitive detection of surface- and size-dependent direct and indirect band gap transitions in ferritin," *Nanotechnology* 25, 135703-135709 (2014).
- ¹² V. V. Nikandrov, et al., "Light induced redox reactions involving mammalian ferritin as photocatalyst," *Journal of Photochemistry and Photobiology B-Biology* 41, 83-89 (1997).
- ¹³ D. Ensign, M. Young, and T. Douglas, "Photocatalytic synthesis of copper colloids from Cu(II) by the ferrihydrite core of ferritin," *Inorganic Chemistry* 43, 3441-3446 (2004).
- ¹⁴ K. Ageishi, T. Endo, and M. Okawara, "Hydrogen Evolution from Water by Use of Viologen Polymers as Electron Transfer Catalyst," *Journal of Polymer Science* **19**, 1085-1090 (1981).
- ¹⁵ Y. Amao and Ichiro Okura, "Photoinduced hydrogen production with the system containing water-soluble viologen-linked porphyrins and hydrogenase," *Journal of Molecular Catalysis* **17**, 9-21 (2002).
- ¹⁶ L. Cao and Y. Wang, "Photocatalysis of viologens for photoinitiated polymerization using carboxylic acid as electron donors," *Journal of Photochemistry and Photobiology A: Chemistry* **333**, 63-69 (2017).

-
- ¹⁷T. Cedervall et al., “Understanding the nanoparticle-protein corona using methods to quantify exchange rates and affinities of proteins for nanoparticles,” *Proceedings of the National Academy of Sciences of the United States of America* **104**, 2050-2055 (2007).
- ¹⁸ O.H. Lowry, et al., “Protein Measurement with the Folin Phenol Reagent,” *J. Biol. Chem.* **193**, 265-275 (1951).
- ¹⁹ K. R. Hansen, “Ferritin encapsulated PbS, PbSe, and MoS₂ Nanocrystals for Photovoltaic Applications,” Senior Thesis, Brigham Young University (2017).
- ²⁰ F. A. A. Rajathi and V.R.M. S. Nambaru, “Phytofabrication of nano-crystalline platinum particles by leaves of *Cerbera manghas* and its antibacterial efficacy,” *International Journal of Pharma and Bio Sciences* **5**, 619-628 (2014).
- ²¹ N. V. et. al., “Synthesis and characterization of Pt-Pd alloy and core-shell bimetallic nanoparticles for direct methanol fuel cells (DMFCs): Enhanced electrocatalytic properties of well-shaped core-shell morphologies and nanostructures,” *International Journal of Hydrogen Energy* **36**, 8478-8491 (2011).
- ²² G. L. Peterson, “Determination of total protein,” *Methods in Enzymology* **91**, 95-119 (1983).
- ²³ R. Robert and A. H. Richards, “Interference by Tris buffer in the estimation of protein by the Lowry procedure,” *Analytical Biochemistry* **62**, 240-247 (1974).
- ²⁴ M. M. Bradford, “A Rapid and Sensitive Method for the Quantitation of Microgram Quantities of Protein Utilizing the Principle of Protein-Dye Binding,” *Analytical Biochemistry* **72**, 248-254 (1976).
- ²⁵ G.L. Peterson, “A Simplification of the Protein Assay Method of Lowry *et al.* Which is More Generally Applicable,” *Analytical Biochemistry* **83**, 346-356 (1977).